Missouri University of Science and Technology
Scholars' Mine

Chemistry Faculty Research & Creative Works | Chemistry

11 Apr 2022

Theranostic Copolymers Neutralize Reactive Oxygen Species and Lipid Peroxidation Products for the Combined Treatment of Traumatic Brain Injury

Aaron Priester

Richard Waters

Ashleigh Abbott

Krista Hilmas

et. al. For a complete list of authors, see https://scholarsmine.mst.edu/chem_facwork/3199

Follow this and additional works at: https://scholarsmine.mst.edu/chem_facwork

 Part of the Chemistry Commons, and the Materials Science and Engineering Commons

Recommended Citation

A. Priester and R. Waters and A. Abbott and K. Hilmas and K. Woelk and H. A. Miller and A. W. Tarudji and C. C. Gee and B. McDonald and F. M. Kievit and A. J. Convertine, "Theranostic Copolymers Neutralize Reactive Oxygen Species and Lipid Peroxidation Products for the Combined Treatment of Traumatic Brain Injury," *Biomacromolecules*, vol. 23, no. 4, pp. 1703 - 1712, American Chemical Society, Apr 2022.
The definitive version is available at https://doi.org/10.1021/acs.biomac.1c01635

This Article - Journal is brought to you for free and open access by Scholars' Mine. It has been accepted for inclusion in Chemistry Faculty Research & Creative Works by an authorized administrator of Scholars' Mine. This work is protected by U. S. Copyright Law. Unauthorized use including reproduction for redistribution requires the permission of the copyright holder. For more information, please contact scholarsmine@mst.edu.

pubs.acs.org/Biomac

Article

Theranostic Copolymers Neutralize Reactive Oxygen Species and Lipid Peroxidation Products for the Combined Treatment of Traumatic Brain Injury

Aaron Priester, Richard Waters, Ashleigh Abbott, Krista Hilmas, Klaus Woelk, Hunter A. Miller, Aria W. Tarudji, Connor C. Gee, Brandon McDonald, Forrest M. Kievit, and Anthony J. Convertine*

Cite This: *Biomacromolecules* 2022, 23, 1703−1712

Read Online

ACCESS | Metrics & More | Article Recommendations | Supporting Information

ABSTRACT: Traumatic brain injury (TBI) results in the generation of reactive oxygen species (ROS) and lipid peroxidation product (LPOx), including acrolein and 4-hydroxynonenal (4HNE). The presence of these biochemical derangements results in neurodegeneration during the secondary phase of the injury. The ability to rapidly neutralize multiple species could significantly improve outcomes for TBI patients. However, the difficulty in creating therapies that target multiple biochemical derangements simultaneously has greatly limited therapeutic efficacy. Therefore, our goal was to design a material that could rapidly bind and neutralize both ROS and LPOx following TBI. To do this, a series of thiol-functionalized biocompatible copolymers based on lipoic acid methacrylate and polyethylene glycol monomethyl ether methacrylate (FW ∼ 950 Da) (O950) were prepared. A polymerizable gadolinium-DOTA methacrylate monomer (Gd-MA) was also synthesized starting from cyclen to facilitate direct magnetic resonance imaging and in vivo tracking of accumulation. These neuroprotective copolymers (NPCs) were shown to rapidly and effectively neutralize both ROS and LPOx. Horseradish peroxidase absorbance assays showed that the NPCs efficiently neutralized H_2O_2, while R-phycoerythrin protection assays demonstrated their ability to protect the fluorescent protein from oxidative damage. ^{1}H NMR studies indicated that the thiol-functional NPCs rapidly form covalent bonds with acrolein, efficiently removing it from solution. In vitro cell studies with SH-SY5Y-differentiated neurons showed that NPCs provide unique protection against toxic concentrations of both H_2O_2 and acrolein. NPCs rapidly accumulate and are retained in the injured brain in controlled cortical impact mice and reduce post-traumatic oxidative stress. Therefore, these materials show promise for improved target engagement of multiple biochemical derangements in hopes of improving TBI therapeutic outcomes.

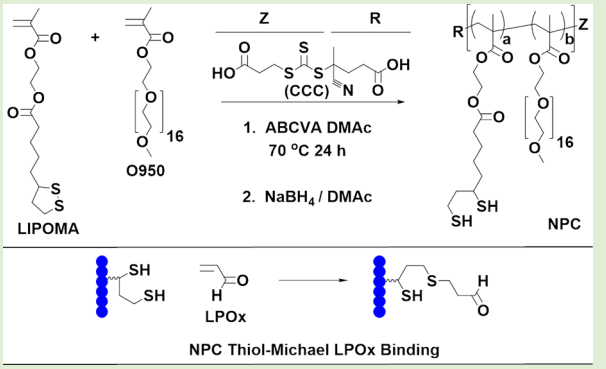

1. INTRODUCTION

Traumatic brain injury (TBI) is a major cause of disability and death among children and young adults. Damage from a TBI occurs in two separate phases, which consist of the initial brain trauma and a secondary phase.[1,2] During the secondary phase, reperfusion injury, delayed cortical edema, and blood−brain barrier (BBB) breakdown can result in the release of reactive oxygen species (ROS), calcium imbalances, and the production of highly reactive lipid peroxidation products.[3,4] During the secondary phase, which progresses over the course of days to weeks, this release of ROS, calcium, and lipid peroxidation products leads to increased cytokine and chemokine expression as well as the formation of chronically reactive astrocytes and activated microglia.[5] These biochemical and cellular cascades lead to neural degeneration and progression of tissue damage into other regions of the brain. As a result, many of the lifelong problems that arise following a TBI can at least partially be attributed to mechanisms that occur following the initial brain trauma.[6] Current therapies provide only palliative support for TBI patients, highlighting the need for new therapeutic agents that are capable of minimizing neurodegeneration during the secondary phase of the injury.[7−10] Several antioxidant therapies have been investigated, including poly(ethylene glycol) (PEG)-conjugated superoxide dismutase,[11] PEG-conjugated catalase,[12] tirilazad,[13] as well as combinations of these agents. Although these antioxidant materials have shown promise in preclinical studies, they have failed to improve the patient outcome in large clinical studies.

Received: December 15, 2021
Revised: March 9, 2022
Published: March 22, 2022

Downloaded via MISSOURI UNIV SCIENCE & TECHNOLOGY on February 21, 2023 at 20:43:46 (UTC).
See https://pubs.acs.org/sharingguidelines for options on how to legitimately share published articles.

ACS Publications

© 2022 American Chemical Society

Scheme 1. Synthetic Strategy for the RAFT Synthesis of NPCs Blocked with MRI Contrast GdMA Using Isolated LIPOMA-co-O950 NPC Series Macro-CTA and the Proposed Mechanism for Covalent Neutralization of Lipid Peroxidation Products[a]

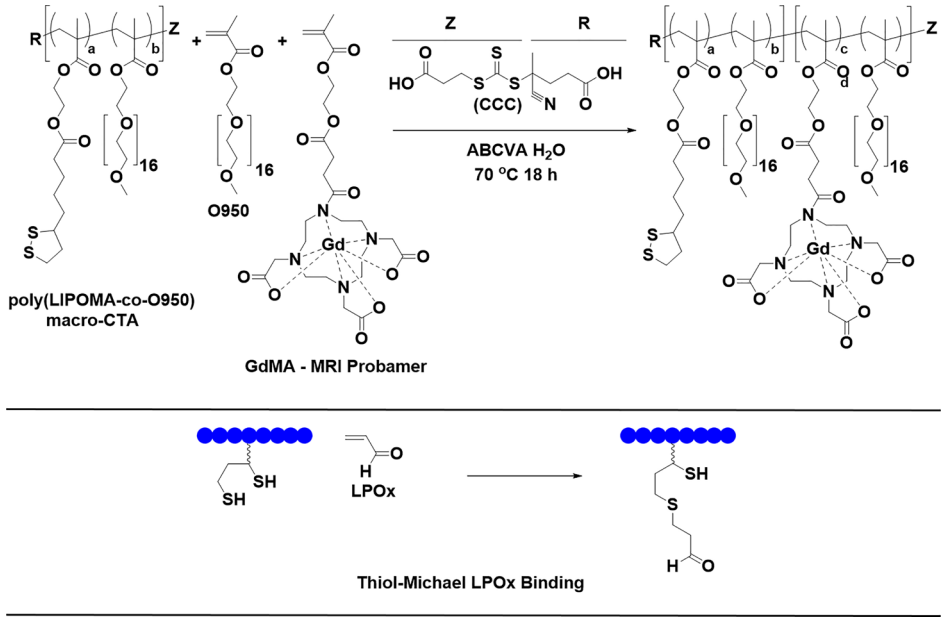

[a]Disulfide bonds were reduced to thiols by reacting the purified block copolymer $NaBH_4$ in DMAc. LIPOMA-co-O950 NPC series macro-CTAs without GdMA were directly reduced with $NaBH_4$, purified, and tested. All LIPOMA-co-O950 macro-CTAs were RAFT synthesized in DMAc at 70 °C for 24 h using CCC and ABCVA.

These failed clinical trials stem from numerous drawbacks of current therapies, which include (1) poor delivery into the brain, leading to minimal target engagement; (2) incomplete understanding of the disease process, leading to suboptimal patient selection; and (3) effectiveness against only one of the many therapeutic targets, leading to reduced treatment efficacy. As a result, there is a critical need to develop new therapies that are capable of improved brain delivery, robust efficacy against a broad patient population, and the ability to neutralize multiple reactive species associated with the secondary phase of TBI. Such therapies could provide substantial long-term physical, behavioral, and psychosocial benefits for individuals who have sustained a TBI.

Previously, we detailed the development of oxygen reactive polymers (ORPs) and antioxidant nanoparticles that are able to act as both a diagnostic magnetic resonance imaging contrast agent and a therapeutic ROS sponge.[14−16] These ORPs, which were prepared by reversible addition−fragmentation chain transfer (RAFT) polymerization, contain thioether residues as the ROS scavenging agent and O950 residues to increase circulation half-life and biocompatibility. Gadolinium (Gd) contrast agents for MRI analysis were then added post-polymerization. These materials were shown to effectively accumulate in the damaged brain and reduce histological measures of secondary injury in a controlled cortical impact (CCI) mouse model of TBI. Thiols are another class of antioxidant sulfur compound that rapidly react with free radicals.[17] Additionally, thiols also readily react with electron-deficient alkenes via thiol-Michael addition reactions.[18] The result of this reaction is the formation of a thioether linkage and the conversion of the highly reactive alkene into an alkane. In these studies, we describe the development of a new series of theranostic polymers that contain thiol residues that are capable of neutralizing both ROS and LPOx.

In these studies, our objective was to develop neuroprotective copolymers (NPCs) that can efficiently neutralize both ROS and LPOx. In order to accomplish this objective, a series of hydrophilic copolymers containing thiol residues derived from lipoic acid (LA) were synthesized. LA is an endogenous organosulfur compound that is an essential cofactor for several mitochondrial enzymes.[19] Both LA and dihydrolipoic acid (DHLA) are capable of scavenging $^{\bullet}OH$ radicals, but only DHLA is capable of scavenging superoxide radical anions, suggesting that DHLA is an excellent antioxidant.[20] LA was selected as the thiol source as this compound: (1) contains a carboxylic acid with which to attach the methacrylate group, (2) is commercially available and inexpensive, and (3) contains two sulfhydryl residues as a disulfide group.

The latter point is necessary for the subsequent polymerization of the monomer as free thiol groups efficiently inhibit free radical polymerizations. LA was first converted into a methacrylate monomer (LIPOMA) via carbodiimide-mediated esterification with 2-hydroxyethyl methacrylate. LIPOMA was then copolymerized with PEG methacrylate (FW ∼ 950 Da) (O950) to prepare a series of NPCs. Our previous studies have shown that the large PEG macromonomer can be used to prepare biocompatible copolymers with favorable PK/biodistribution profiles.[21−23]

The LIPOMA-containing NPCs were then reduced with sodium borohydride to yield two thiol residues per mole of LIPOMA comonomer. Our hypothesis here was that the thiol groups could serve two neuroprotective functions by both rapidly neutralizing ROS and effectively forming covalent bonds with LPOx via thiol-Michael reactions. RAFT polymerization methodology was employed in order to yield copolymers with controlled molecular weights and narrow molar mass dispersities (Đ). To evaluate the aqueous morphology of the NPCs, a series of polymers with increasing

https://doi.org/10.1021/acs.biomac.1c01635
Biomacromolecules 2022, 23, 1703−1712

molar feed ratios of the hydrophobic LIPOMA comonomer were synthesized. These ratios were selected in order to yield copolymers that were below the renal clearance molecular weight. Additionally, a 20 wt % poly(LIPOMA-*co*-O950) macro-CTA was co-blocked with GdMA (contrast agent) and O950 for MRI studies (Scheme 1).

2. MATERIALS AND METHODS

2.1. Materials. The following chemicals were obtained from Chem Impex Int'l: DL-α-LA (99.37%), 4-dimethylaminopyridine (DMAP, 99.43%), 3-(3-dimethylaminopropyl)-1-ethyl-carboiimide hydrochloride (99.9%), copper(II) chloride (98.47%), ascorbic acid (99.75%), bromoacetic acid *tert*-butyl ester (99.35%), cyclen (99.6%), dichloromethane (99.91%), dimethyl sulfoxide (DMSO, 99.99%), *N*,*N*-dimethylacetamide anhydrous (DMAc, 99.93%), 5, 5′-dithiobis(2-nitrobenzoic acid) (Ellman's reagent, 99.56%), and trifluoroacetic acid (TFA, 99.9%). O950 [poly(ethylene glycol) methyl ether methacrylate], Gd(III) chloride hexahydrate (99.9%), mono-2-(methacryloyloxy)ethyl succinate (SMA), sodium acetate trihydrate (>99.5%), L-cysteine, 4,4′ azobis (4-cyanovaleric acid) (ABCVA, >98%), 2,2′-azobis(2-methyl-propionamindine) dihydrochloride (AAPH, 97%), Chelex 100 sodium form resin, phenol red (95%), reduced LA, deuterated DMSO (99.9 at %), and deuterium oxide (D_2O 99.8 at %) were obtained from Sigma-Aldrich. 2-Hydroxymethacrylate (HEMA, stab. with 4-methoxyphenol, >97%), horseradish peroxidase (HRPO), and acrolein diethyl acetal (ADA, 96%) were obtained from Alfa Aesar. CCC (95%) was obtained from Boron Molecular. Sodium borohydride (>95%) and oxalyl chloride (>98%) were obtained from TCI. R-phycoerythrin protein (RPE) was obtained from Cayman Chemical Company. DMEM/F12 1:1 cell media and fetal bovine serum (FBS) were obtained from HyClone. Pen Strep was obtained from Gibco.

2.2. Methods. *2.2.1. Synthesis of NPC Series Copolymers.* LIPOMA monomer was synthesized in preparation for these copolymerizations. LIPOMA synthesis procedure can be found in the Supporting Information along with the corresponding $^1H/^{13}C$ NMR data (Figure S1). RAFT copolymerizations of LIPOMA and O950 and RAFT homopolymerization of O950 (control) were conducted in DMAc at an initial total comonomer concentration of 40 wt % with a CTA-to-initiator ratio ($[CTA]_o/[I]_o$) of 20 to 1 and a monomer-to-CTA ratio ($[M]_o/[CTA]_o$) of 25 to 1. A series of polymerizations containing between 0 (O950 control, NPC 1) and 50 wt % LIPOMA were synthesized. Polymerization solutions were purged with argon for 30 min and transferred to a preheated water bath at 70 °C for 24 h. Quantitative monomer conversion was confirmed by ^1H NMR in $CDCl_3$ by following the disappearance of vinyl resonances at 5.5 and 6.0 ppm. Copolymer compositions were determined based on monomer conversion as determined by ^1H NMR spectroscopy in $CDCl_3$. Polymers were dialyzed in a Spectrapor regenerated cellulose dialysis membrane against ethanol for one day followed by deionized (DI) water for two days, after which they were freeze-dried. O950 control was dialyzed against DI water only prior to freeze-drying. A representative procedure for the 20 wt % LIPOMA polymer (NPC 3) is as follows: to a 25 mL round bottom flask was added O950 (4.00 g, 4.21 mmol), LIPOMA (1.00 g, 3.10 mmol), 3.59 mL of a 25 mg mL^{-1} CCC stock in DMAc (90 mg, 0.293 mmol), 410 μL of a 10 mg mL^{-1} ABCVA in DMSO (4.1 mg, 0.015 mmol), and DMAc (3.5 g).

2.2.2. Synthesis of Poly[(LIPOMA-co-0950)-b-(O950-co-GdMA)]. GdMA monomer was synthesized in preparation for this block copolymerization. The full GdMA synthesis procedure can be found in the Supporting Information along with the corresponding ^1H NMR data (Figures S2−S4). RAFT copolymerization of GdMA and O950 from a poly(LIPOMA-*co*-0950) macro-CTA was conducted at $[M]_o/[\text{macro-CTA}]_o$ and $[\text{macro-CTA}]_o/[I]_o$ ratios of 8 and 10, respectively. To a 25 mL round bottom flask was added *poly*(LIPOMA-*co*-O950) (20 wt % LIPOMA, NPC 3) (1 g, 0.058 mmol CCC), ABCVA (100 μL of a 16.09 mg mL^{-1} stock in ethanol), GdMA (121 mg, 0.217 mmol), O950 (0.22 g, 0.232 mmol), and DI water (4.15 mL). The polymerization solution was purged with argon for 30 min and transferred to a preheated water bath at 70 °C for 18 h. Following polymerization, the solution was transferred to a Spectrapor regenerated cellulose dialysis membrane, dialyzed against distilled water for three days, and freeze-dried.

2.2.3. Reduction of NPC Series Copolymers with Sodium Borohydride ($NaBH_4$). NPC copolymers were dissolved in DMAc, and $NaBH_4$ was added to reduce disulfides on LIPOMA units to generate thiol residues. After reacting for 24 h, solutions were transferred to a Spectrapor regenerated cellulose dialysis membranes and dialyzed against DI water for three days, periodically adjusting the pH of the dialysis solution to 7.4 with phosphate buffer (200 mM, pH 7.4). Reduced copolymers were then freeze-dried. A representative procedure for NPC 3 reduction is as follows: to a 50 mL test tube, 0.45 g of NPC 3 (0.279 mmol LIPOMA) and 9 mL of DMAc were added. Once dissolved, 0.18 g of $NaBH_4$ (4.76 mmol, 17:1 M ratio) was added and reacted for 24 h. A one-pot procedure was later adopted in which $NaBH_4$ was added directly to the polymerization medium (>99% comonomer conversion) and reacted for 24 h, followed by dialysis and freeze-drying. O950 control (NPC 1) did not undergo this reduction step.

2.2.4. Gel Permeation Chromatography Analysis. Molecular weights and molar mass dispersity values for the copolymer series were determined using the Agilent Infinity II Series gel permeation chromatographer (GPC) with poly(methyl methacrylate) standards and DMF + 1% LiBr as the solvent. Traces for NPC 1, 2, and 3 can be found in Figure S5.

2.2.5. Dynamic Light Scattering Analysis. For the dynamic light scattering (DLS) analysis, 2 mL of a 2 mg mL^{-1} polymer solution in phosphate-buffered saline (PBS) was prepared and was pipetted into Sarstedt 1 × 1 × 4 cm cuvettes. The average hydrodynamic diameters of the copolymer series were determined using DLS measurements obtained from the Malvern Zetasizer Ultra Benchtop Analyzer.

2.2.6. Assay Absorbance and Fluorescence Analysis. Absorbance and fluorescence values for assays were measured using the TECAN Infinite M Nano+ Plate Well Reader. Either BD Falcon 96-well flat transparent plates (absorbance) or Corning flat black 96-well plates (fluorescence) were utilized.

2.2.7. Reduced NPC Series Thiol Quantification. The molar concentration of thiols per gram of copolymer for each copolymer was determined using Ellman's assay. A standard curve was first constructed using L-cysteine as the thiol source.[27] This procedure can be found in the Supporting Information. Stocks of reduced copolymers (10 mg mL^{-1}) in DI water and Ellman's reagent (3 mg mL^{-1}) in pH 7 sodium phosphate buffer were first prepared. The reduced copolymer stock was used to create a series of sample concentrations by diluting 0, 10, 20, 30, or 40 μL of the stock into 3 mL of PBS buffer (100 mM, pH 7.0) followed by 50 μL addition of Ellman's reagent solution to each sample. After 15 min of incubation, 200 μL of each sample was pipetted into a 96-well plate, and absorbance was measured at 412 nm. Using absolute absorbance values and the standard curve, moles of thiols per gram of polymer were calculated and compared to theoretical values (Figure S6).

2.2.8. Quantifying Neutralization of ROS Species H_2O_2 by NPC Series Copolymers Using HRPO Assay. HRPO was used as the mediating species for the oxidation of phenol red by H_2O_2 according to a previously published protocol.[28] Stocks of reduced NPC series polymers (50 mg mL^{-1}), H_2O_2 (2.5 mM using 3% H_2O_2), phenol red (1 mg mL^{-1}), and NaCl (0.5 M) were prepared in distilled water. HRPO stock (0.5 mg mL^{-1}) was prepared in a pH 7 potassium phosphate buffer (10 mM). Phenol red solution (RPS) was then prepared by combining phosphate buffer (5 mL), NaCl solution (14 mL, 140 mM), HRPO stock (5 mL, 50 μg/mL), phenol red stock (5 mL, 0.1 g/L), and distilled water (21 mL). RPS and H_2O_2 concentrations (50 μM) were held constant for all experiments. H_2O_2 and varying concentrations of polymer solutions (0.25−10 mg mL^{-1}) were first incubated prior to RPS addition. This was followed by additions of RPS solution and NaOH to adjust the sample pH to 12.5. Samples (n = 3) were incubated for 5 min, and absorbance was measured at 610 nm. Polymer blanks were also prepared in the same

https://doi.org/10.1021/acs.biomac.1c01635
Biomacromolecules 2022, 23, 1703−1712

manner minus H_2O_2. Reduction in absolute absorbance as a function of copolymer composition (entire NPC series) and incubation time (NPC 3 only) for increasing copolymer concentrations was then determined. A representative procedure for polymer sample preparation at a concentration of 1 mg mL^{-1} is as follows: to a 2 mL tube was added 35 μL of H_2O_2 stock, 35 μL of reduced NPC 3 stock (50 mg mL^{-1}), and 140 μL of DI water. Samples were incubated for 30 min followed by the addition of 1540 μL of RPS and 17.5 μL of 1 M NaOH and measured at 610 nm.

2.2.9. Neutralization of Free Radical Cu by NPC 3 Using RPE Fluorescent Protein Assay. The ability of reduced NPC series copolymers to protect proteins from oxidative damage was evaluated using an RPE assay that was described elsewhere.[29] The assay was standardized using AAPH, the procedure for which is found in the Supporting Information. Stock concentrations of the reduced NPC 3 copolymer and NPC 1 (control O950) were prepared in 150 mM pH 7 phosphate buffer (12.04 mg mL^{-1}), from which a range of copolymer stock concentrations were produced. Thiol concentrations for the reduced polymer were determined using the data obtained from Ellman's reagent assay. Cu free radical solution was prepared 45 min prior to use by combining ascorbic acid (773 μM) and $CuCl_2$ (2.23 μM) in phosphate buffer. RPE control and Cu-only samples were prepared by combining 1978 μL of buffer with 22 μL RPE stock (1.7 μM in buffer). A range of copolymer samples for analysis were prepared by combining 22 μL of RPE stock, 24 μL of the copolymer stocks, and 1954 μL of buffer. Copolymer samples were incubated with the protein prior to Cu addition. Then, 185 μL of each sample (n = 3) was pipetted into a 96-well plate, and fluorescence values (time, t = 0 min) were measured at an excitation of 498 nm and an emission of 575 nm. Following the initial measurement, 15 μL of the Cu radical solution was then added to each well minus the control and blank (15 μL of buffer). Fluorescence was measured immediately and tracked for 30 min. Blanks were subtracted out, and values were normalized to the control. Normalized fluorescence values at each time were divided by the initial (t = 0 min) to obtain the absolute fluorescence for each sample. Reduction of absolute fluorescence as a function of thiol/Cu ratio was then determined.

2.2.10. Quantifying the Effect of Reduced NPC 3 Copolymer on Acrolein Neutralization via Proton NMR. ^{1}H NMR was used to quantify the effect of the reduced NPC 3 copolymer on the neutralization of LPOx acrolein by tracking the reduction in acrolein vinyl resonances with the increase in copolymer concentration. This method was first verified using reduced LA (DHLA), which is found in the Supporting Information. Once verified, a fresh acrolein stock was prepared by combining 200 μL ADA, 600 μL D_2O, and 20 μL TFA. A range of thiol-to-acrolein samples with varying molar ratios (0, 0.2, 0.4, 0.6, 0.8, and 1) were prepared using the reduced copolymer. Acrolein and buffered D_2O volumes were held constant at 80 and 84 μL, respectively. Varying reduced copolymer concentrations were added to this fixed concentration of acrolein, and the total volume was adjusted to 500 μL with additional D_2O. Samples were then incubated at 37 °C and measured using ^{1}H NMR. The integral of the vinyl peaks (6.25−6.75 ppm) was normalized to the ethanol ($HO\mathbf{CH_2}CH_3$) resonance (1.0−1.5 ppm) produced upon the hydrolysis of ADA for each ratio. This ratio was used to calculate the percentage reduction of the vinyl peaks for acrolein compared to the untreated acrolein spectrum. A representative sample for 0.2 thiol-to-acrolein molar ratio for reduced NPC 3 copolymer is as follows: to a 1 mL Eppendorf tube was added 270 μL of D_2O, 84 μL of buffered D_2O, 80 μL of acrolein stock, and 66 μL of reduced polymer stock.

2.2.11. Quantifying the Effect of Reduced NPC 3 Copolymer on SH-SY5Y Cell Viability against ROS Species H_2O_2 and LPOx Product Acrolein Using MTT Assay and Confocal Microscopy. SH-SY5Y cells were cultured in a medium of DMEM/F12 1:1 Dulbecco's modified Eagle's medium + 2.5 mM L-glutamine + 15 mM N-(2-hydroxyethyl)-piperazine-N′-ethanesulfonic acid buffer containing 10% FBS and 1% PenStrep. Cells were seeded in 96-well plates at a density of ∼7500 cells/cm^2 (∼2500 cells per well, 200 μL). Cell differentiation was catalyzed with media (200 μL) containing retinoic acid (10 μM) for two days. The cells were then incubated with regular media for additional four days. Polymer, acrolein, and peroxide toxicity curves were determined for these differentiated cells prior to cell protection studies (Figure S7). Following toxicity studies, a constant copolymer concentration of 0.3 mg mL^{-1} was used for cell viability assays, while H_2O_2 concentrations (40−250 μM) and acrolein concentrations (2.5−25 μM) were varied. After seeded cells (2500 cells/well) were differentiated, the cells were incubated with polymer for 15 min prior to acrolein or H_2O_2 addition. The treated cells were then incubated for 18 h before removing media, washing with PBS, and replacing with 100 μL of the new media. MTT (10 μL, 5 mg mL^{-1} in PBS buffer) was added to each well and incubated for 4 h before the addition of the solubilization solution to dissolve the formazan crystals. In addition, negative (untreated cells) and positive controls (cells + 2000 μM H_2O_2) were also prepared. Solutions were incubated overnight, and absorbance was then measured at 600 nm. The percentage viability was determined by referencing the absolute absorbance of samples to that of the negative control. These data were then compared to those for the cells treated with H_2O_2 or acrolein but no polymer. Treated and untreated cells were stained with Hoescht and Galectin 3 antibody and imaged on the Nikon confocal microscope.

2.2.12. Controlled Cortical Impact Mouse Model of TBI. All animal procedures were performed in accordance with the approval of the University of Nebraska−Lincoln IACUC. Six to eight week old male C57BL/6J mice (Jackson Laboratory, Bar Harbor, ME, USA) were acclimated for one week prior to the procedures. Mice were anesthetized with 3% isoflurane gas via inhalation and were maintained at ∼1.5% with a nose cone on a stereotaxic frame (David Kopf Instruments, Tujunga, CA, USA). The hair of the scalp was removed with Nair (Church and Dwight Co., Inc., Princeton, NJ, USA), and the scalp was disinfected with a Betadine scrub and isopropanol wipes afterward. Lidocaine (0.05 mL of 5 mg/mL) and bupivacaine (0.05 mL of 0.3 mg/mL) were applied to the scalp, and buprenorphine SR (60 μL of 0.5 mg/mL) was given subcutaneously. An approximately 1 cm midline incision was made on the scalp over bregma. An approximately 2 mm craniectomy was made in the skull over the left frontoparietal cortex (2 mm anterior and 2 mm left of lambda) using a surgical drill. A controlled cortical impactor (Hatteras Instruments, Cary, NC, USA) attached to the stereotaxic frame with a 2 mm convex tip was used to impact the brain normal to the dura surface at a depth of 2.5 mm, a velocity of 4 m/s, and a dwell time of 80 ms. Any bleeding was controlled, and incisions were closed using tissue adhesive.

2.2.13. In Vivo Dynamic Contrast-Enhanced Magnetic Resonance Imaging. Roughly 3 h following CCI, dynamic contrast-enhanced magnetic resonance imaging (DCE-MRI) was performed to assess the accumulation of NPC 3 across the disrupted BBB. All experiments were approved by the University of Nebraska−Lincoln IACUC. Mice (n = 4) were anaesthetized using about 1.5% isoflurane, adjusted to maintain breathing between 40 and 80 breaths per minute. K^{trans} imaging was performed similarly to previously published work.[1,2] Imaging took place using a 9.4T MRI system (Varian, Palo Alto, CA) with a 4 m Millipede RF imaging probe with triple-axis gradients (100 G cm-1 max). Separate baseline gradient echo scans were performed with flip angles (FAs) of 10 and 30° using the following parameters: TR = 54.28 ms, TE = 2.73 ms, data matrix = 128 × 128, field of view = 20 × 20 × 10 mm3 split into ten 1 mm slices, and 5 averages for a scan time of 34 s. Mice were injected with 100 μL NPC 3 stock (4 mg mL^{-1}) via a tail vein catheter followed with 100 μL of PBS to flush ensure administration of the entire NPC 3 dose. After contrast administration, 30° gradient echo scans were performed serially over the course of 45 min using the same parameters listed above, resulting in about 70 postcontrast scans per animal. Following data acquisition, processing was performed using a custom MATLAB script developed in house. R_1 mapping was completed via the variable flip angle method using the following equation

$$S_{SPGR}/\sin(\alpha) = S_{SPGR}/\tan(\alpha)\cdot E_1 + M_0\,(1 - E_1)$$

where α is FA, SSPGR is the signal intensity, E_1 is exp(TR/T1−), and M_0 is a proportionality constant related to longitudinal magnetization.

https://doi.org/10.1021/acs.biomac.1c01635
Biomacromolecules 2022, 23, 1703−1712

Concentration maps were estimated by comparing baseline R_1 maps with postcontrast R−1 maps based on the following equation

$$C(t) = (R_1(t) - R_{10})/r_1$$

where C is the NPC 3 concentration at time t postinjection, R−1(t) is the R_1 value at time t, R_{10} is the baseline R_1 value, and r_1 is the T_1 relaxivity of NPC 3. K^{trans} maps were generated based on the Patlak model.[4] This model compares the NPC 3 contrast within tissue and blood, assuming a unidirectional diffusion across the BBB during the acquisition time to estimate the blood-to-brain transfer coefficient, K^{trans}, describing the transport of NPC 3 from the blood to the extravascular extracellular space. Fitting used the following equation: {Nation, 2019 #143}

$$C_{tissue}(t) = K^{trans}\int_0^t [C_{blood}(u)du] + v_p \cdot C_{blood}(t)$$

where C_{tissue} and C_{blood} are NPC 3 concentrations in the tissue and blood, respectively, and v_p is the intravascular blood volume fraction.

Following K^{trans} mapping, ROIs were drawn on structural images over the injured cortical region as well as over the non-damaged hemisphere, and mean values were calculated. Data presented are the mean K^{trans} values from each mouse over the primary injured region in a single slice and over the contralateral hemisphere averaged across all slices displaying injury.

2.2.14. Dihydroethidium Histological Analysis. The NPC 3 group was treated with a tail vein injection of NPC 3 in Dulbecco's phosphate buffered saline (DPBS, Thermo Fisher Scientific, Waltham, MA) (100 μL of 2 mg mL^{-1}) immediately after the surgery, while the MnTMPyP group was treated with an intraperitoneal injection of Mn(III)tetrakis(1-methyl-4-pyridyl)porphyrin (MnTMPyP, 475 872, Sigma-Aldrich, St. Louis, MO) in DPBS (500 μL of 1 mg/mL) immediately after the surgery. The size of each treatment group is three mice. A dihydroethidium (DHE, Thermo Fisher Scientific) assay was performed as previously described with modifications.5 Briefly, DHE was dissolved in DMSO before further dilution in DPBS. DHE (125 μL of 5 mg/mL) was injected through the tail vein into each mouse at 3 h post-CCI. Mice were transcardially perfused at 1 h after DHE injection with ice-cold 4% paraformaldehyde (PFA) in 0.1 M phosphate buffer pH 7.5. Brain tissue was collected, trimmed, and fixed in 4% buffered PFA for 24 h. The brains were moved into 30% sucrose in DPBS for 3 d at 4 °C for cryoprotection. The brains were then embedded in 2.6% carboxymethylcellulose (CMC, C4888, Sigma-Aldrich), frozen on dry ice, and sliced coronally at a 15 μm thickness with cryotome (Leica Biosystems, Wetzlar, Germany). The brain slices were laid on a poly-L-lysine-coated microscope slide (Thermo Fisher Scientific) and dried overnight at RT. Sections were washed with DPBS 3 times for 5 min each to remove the CMC, followed by water, and ProLong Gold Antifade Mountant (Thermo Fisher Scientific) was applied. Images were acquired with confocal microscopy (LSM800, Zeiss) at an excitation wavelength of 488 nm, an emission wavelength of 560−635 nm, and a 5× objective lens magnification. Quantitative fluorescence intensity analysis was performed with ImageJ software on the perilesional and the contralateral hemispheres.

2.2.15. Statistical Analysis. K^{trans} data were displayed as mean ± standard deviation. Ipsilateral and contralateral groups were compared using a paired t-test with GraphPad Prism 8 software (CA, USA). The DHE quantification data were expressed as mean ± standard error of the mean (SEM). A $p < 0.05$ was considered statistically significant. The DHE quantification was analyzed with one-way ANOVA and Tukey's post hoc test with GraphPad Prism 7 software.

3. RESULTS AND DISCUSSION

3.1. Molecular Weights, Molar Mass Dispersity, and Particle Sizes for NPC Series Copolymers. As can be seen in Table 1, a series of copolymers with compositions ranging from 0 to 50 wt % LIPOMA were prepared.

Table 1. Molecular Weight and Composition Data for Poly(LIPOMA-*co*-O950) Copolymers Prepared by RAFT Copolymerization

NPC	Target wt % LIPOMA	M_n theory (Da)	M_n Exp. (Da)	molar mass dispersity (Đ)	D_H (nm)
1	0	24 000	24 000	1.17	7.0
2	10	20 500	28 000	1.18	5.0
3	20	17 400	26 700	1.25	9.0
4	30	15 300	28 100	1.28	14
5	40	13 700	29 700	1.35	14
6	50	12 400	27 900	1.40	19

These materials displayed relatively narrow molar mass dispersities and molecular weights that were generally consistent with theory. For example, NPC 3 with an initial LIPOMA feed percentage of 20 wt % was determined to have a molecular weight and molar mass dispersity of 26·700 Da and 1.25, respectively. The molecular weight values compare favorably with the theoretical value of 17·400 Da, with deviations likely arising from the use of polymethyl methacrylate standards. Representative procedures for the synthesis, purification, and characterization of these materials can be found in the Supporting Information along with GPC traces for NPC 1, 2, and 3. Analysis of the NPC thiol content was then quantified using Ellman's assay. Here, fair agreement between the experimental thiol concentrations relative to the theoretical values based on LIPOMA content were observed (Figure S6). For example, NPC 3 with a LIPOMA concentration of 20 wt % was found to contain 0.0008 mol of sulfhydryl groups per g of polymer compared to the maximum theoretical sulfhydryl concentration 0.0013 mol per g of polymer for this composition. Here, steric constraints likely reduced the ability of Ellman's reagent to place bulky 2-nitro-5-thiobenzoate groups on thiol groups at both carbon 6 and the nearby carbon 8. To streamline NPC synthesis, one-pot conditions were then developed in which disulfide reductions were conducted directly in the polymerization medium without the intervening purification steps. Because all polymerizations achieved greater than 99.9% monomer conversion, it was hypothesized that an atom-efficient one-pot procedure could be established without noticeable differences in the reduction efficiency. Indeed, GPC analysis combined with thiol quantification via Ellman's assay confirmed the viability of the one-pot procedure. Particle sizes were then determined for the NPCs in pH 7.4 PBS via DLS. These studies showed that NPCs with up to 20 wt % have sizes that are consistent with those of molecularly dissolved unimers (e.g., D_H < 10 nm), while higher LIPOMA feed ratios showed larger particle sizes, suggesting the formation of nanoparticles (D_H > 10 nm) (Table 1).

3.2. Effective Neutralization of ROS Species H_2O_2, Free Radical Cu, and LPOx Product Acrolein Using NPC Series Copolymers. To quantify the ability of the NPCs to neutralize ROS, a simple high-throughput assay based on the HRPO-mediated oxidation of phenol red in the presence of H_2O_2 was conducted. The oxidation of phenol red by H_2O_2 in the presence of HRP yields a deep purple color with a high absorbance at 610 nm. This assay provides a convenient method by which the NPC antioxidant activity can be monitored simply by following the absorbance of phenol red at 610 nm. As can be seen in Figure 1a, all LIPOMA-containing copolymers demonstrated a concentration-depend-

https://doi.org/10.1021/acs.biomac.1c01635
Biomacromolecules 2022, 23, 1703−1712

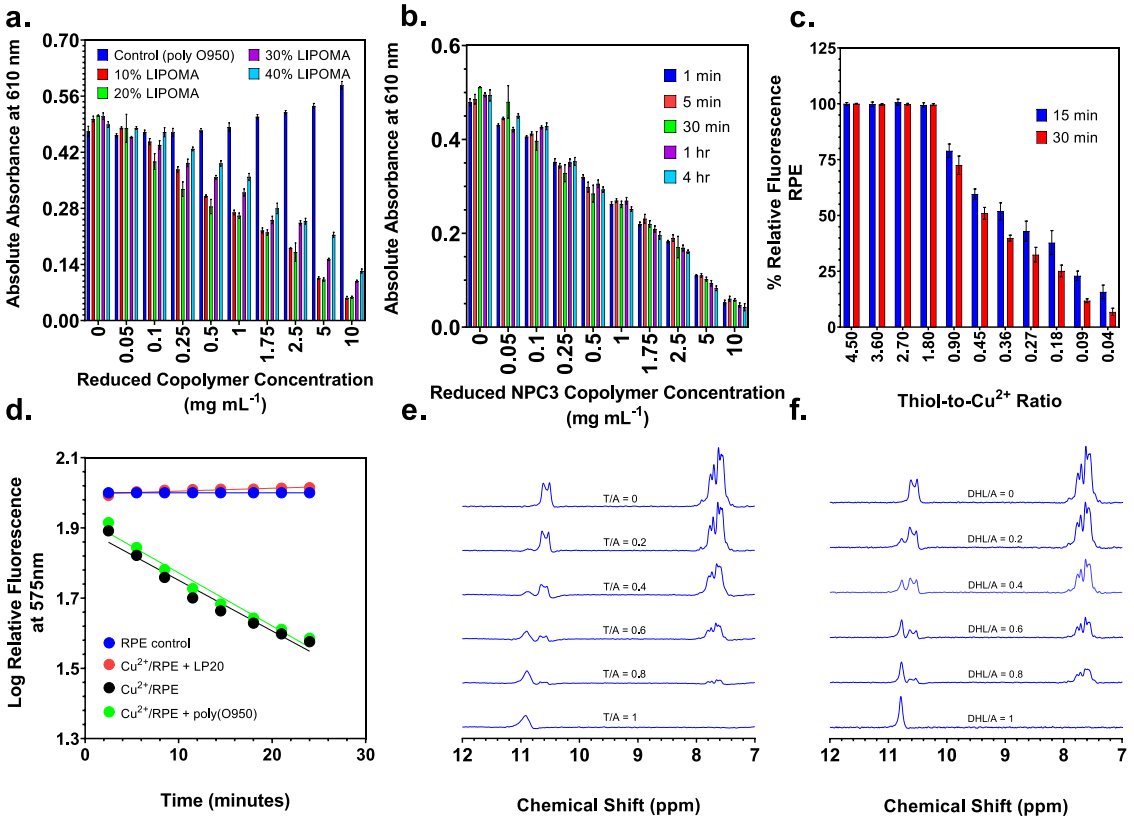

Figure 1. (a) Absolute absorbance values as a function of NPC composition and concentration in HRPO assays. (b) Reduction in absolute absorbance values as a function of incubation time and concentration for the NPC 3 copolymer in HRPO assays. (c) RPE protein analysis of polymer-induced neutralization of free radicals produced by the Fenton reaction between ascorbic acid and Cu^{2+}, illustrated by the reduction in relative fluorescence values as a function of decreasing the thiol/Cu^{2+} ratio. (d) Relative fluorescence as a function of time for RPE incubated with and without reduced NPC 3 and the negative control poly(O950) polymer. ^1H NMR studies conducted in D_2O show that thiol groups react with LPOx alkenes via thiol-Michael reactions, resulting in the formation of thioether adducts between acrolein and (e) DHLA sodium salt or (f) NPC 3 copolymer. Three samples (n = 3) were run for each concentration in HRPO and RPE assays. Average and standard deviations were determined for each concentration from the three samples.

ent ability to reduce the oxidation of phenol red by HRPO-H_2O_2.

As expected, the poly(O950) negative control polymer lacking LIPOMA residues showed no ability to prevent the oxidation of phenol red. In contrast, NPC 2 and 3, which contain 10 and 20 wt % LIPOMA, respectively, reduced the absorbance at 610 nm by 85 and 95%, respectively, at a copolymer concentration of 10 mg mL^{-1}. Interestingly, copolymers containing 30 and 40 wt % LIPOMA were less efficient at reducing phenol red oxidation than copolymers containing 10 and 20 wt % LIPOMA. Here, NPCs 4 and 5 (containing 30 and 40 wt % LIPOMA) reduced phenol red oxidation by 80 and 70%, respectively, relative to polymer-free samples. While all NPCs showed potent antioxidant behavior in this assay, these results suggest that copolymers containing higher concentrations of the hydrophobic LIPOMA comonomer may be forming self-assembled structures that are less accessible to the oxidizer. Based on these results, the 20 wt % copolymer (NPC 3) was selected for all further studies. We next evaluated the antioxidant ability of NPC 3 as a function of time by preincubating the copolymer with H_2O_2 for different periods of time prior to the addition of phenol red. As can be seen in Figure 1b, the copolymer shows a clear concentration-dependent ability to reduce the absorbance of phenol red oxidation. Also evident from this plot is that the antioxidant properties of this copolymer are not especially time-dependent with copolymers preincubated with H_2O_2 for 4 h prior to the introduction of phenol red, showing comparable values to those preincubated for only 1 min. This result is encouraging as it suggests that the copolymers could provide immediate ROS protection following a TBI.

To further confirm the ability of NPC 3 to protect against ROS-mediated damage, we next conducted an assay using the fluorescent protein RPE. This assay is based on the high sensitivity of RPE to ROS-mediated damage, where a rapid and complete reduction in fluorescence is observed when the protein is incubated with a range of oxidizing agents. In this study, free radicals were generated by mixing ascorbic acid with Cu^{2+} salts. Although ascorbic acid is typically considered an antioxidant, it can also undergo a Fenton reaction with copper ions, resulting in the generation of free radicals. The resultant free radicals efficiently oxidize RPE, resulting in a rapid reduction fluorescence. NPC 3-mediated ROS neutralization should protect the protein from oxidation, thus preserving its fluorescent properties. Shown in Figure 1c are fluorescence values at 575 nm for RPE incubated with NPC 3 in a range of thiol/Cu^{2+} concentrations for incubation times of 15 and 30 min. Here, NPC 3 showed concentration-dependent preservation of RPE fluorescence with thiol/Cu^{2+} ratios equal to 1.79 or greater providing complete protection. As the thiol/Cu^{2+} ratio is lowered below unity, a progressive loss in RPE fluorescence is observed. For example, a thiol/Cu^{2+} ratio of 0.9

https://doi.org/10.1021/acs.biomac.1c01635
Biomacromolecules 2022, 23, 1703−1712

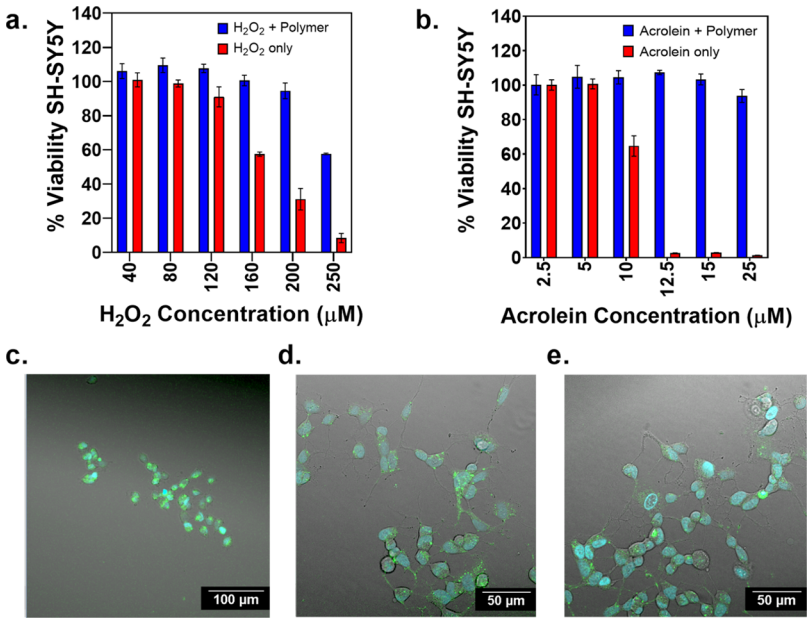

Figure 2. % SH-SY5Y cell viability for neuroblastoma differentiated cells as a function of increasing (a) peroxide and (b) acrolein concentration with and without reduced poly(LIPOPMA-*co*-O950) (0.3 mg/mL). Cells were either left untreated, treated with acrolein, or treated with polymer and acrolein prior to the determination of cell viability via MTT. Optical microscopy images were taken for (c) cells treated with acrolein, (d) cells incubated with the NPC 3 copolymer prior to acrolein addition, and (e) untreated cells. Three trials (n = 3) were run at each concentration in triplicate for MTT viability protection assays. Standard deviations for each concentration were determined using the averages of the three trials.

yields RPE fluorescence values of 79 and 72% at 15 and 30 min, respectively, relative to Cu^{2+} free controls. In contrast, the control polymer [poly(O950), NPC 1] shows a rapid time-dependent decrease in fluorescence that is nearly identical to decreases observed for RPE plus oxidizer alone samples (Figure 1d). These results taken together provide direct evidence that NPC 3 is able to protect the ROS-sensitive proteins from oxidative damage.

Having established the ability of NPC 3 to protect against ROS-mediated damage, we next evaluated this material to neutralize LPOx products by reacting with these species. The electron-deficient double bonds of LPOx were hypothesized to undergo thiol-Michael reactions with the thiol-functional copolymer. In order to provide support for this hypothesis, the reaction between acrolein and NPC 3 was monitored directly in D_2O by ^1H NMR. Because of the highly unstable nature of acrolein, this compound was generated immediately prior to these studies by acid-mediated hydrolysis of acrolein diethyl acetal. Cleavage of the acetal group under acidic conditions proceeds, rapidly generating the aldehyde group and 2 M equivalents of ethanol. The stock solution of acrolein was then diluted in phosphate-buffered D_2O at pH 7.4. In order to compare between samples, the vinyl and aldehyde resonances were normalized to the ethanol methylene resonance ($HO\mathbf{CH_2}CH_3$) at 1.0−1.5 ppm (not shown). The results of these studies can be seen in Figure 1e,f, where the acrolein vinyl resonances located around 7.5 ppm are clearly visible at a thiol-to-acrolein molar ratio of 0 (no copolymer added). Also visible is the acrolein aldehyde proton located around 11 ppm, which changes shape but remains roughly constant in area upon reaction with the copolymer. In contrast, the acrolein vinyl resonances, which are converted into aliphatic thiol-ether groups upon reaction with sulfhydryl groups, showed a progressive reduction in area upon incubation with the increase in sulfhydryl/acrolein ratios. Complete disappearance of the acrolein vinyl resonance was observed for the reduced copolymer at a thiol/acrolein ratio of 1 (Figure 1e). It should also be noted that ^1H NMR analysis was conducted immediately upon mixing the copolymer with the acrolein solution. This suggests that the reaction between the sulfhydryl-functional copolymer and acrolein proceeds rapidly, which is consistent with the proposed thiol-Michael mechanism. For comparison, Figure 1f shows the reaction of acrolein with commercially procured DHLA as a control. Here, a similar trend was observed where the area of the acrolein aldehyde resonance remained roughly constant as the thiol group concentration was increased while the vinyl resonance showed a concentration-dependent reduction in area. These results provide direct evidence that NPC 3 rapidly reacts with LPOx products, potentially inactivating their neuro-destructive properties.

3.3. Protection of SH-SY5Y Cells from ROS and LPOx Products Using the Reduced NPC Copolymer. Based on the ability of NPC 3 to neutralize both ROS and LPOx products, we next evaluated the ability of the copolymer to protect neuron-like SH-SY5Y cells from these biochemical derangements. As shown in Figure 2a, cells treated with H_2O_2 began to show significant toxicity between 120 and 200 μM with a reduction in cell viability from 91 ± 2 to 29 ± 6%, respectively, and nearly complete cell death at 250 μM.

In comparison, cells preincubated with NPC 3 prior to H_2O_2 addition showed significantly higher viability over the same concentration range. Here, nearly complete cell viability relative to untreated controls was observed even at a peroxide concentration of 200 μM. Some cell viability loss was observed at the highest H_2O_2 concentration tested (250 μM); however, the polymer still provided significant improvements relative to the untreated controls (i.e., 58 ± 0.4 vs 9 ± 2%). Similarly, cells treated with acrolein alone over a concentration range of 2.5−25 μM showed a precipitous loss in viability from 100%

https://doi.org/10.1021/acs.biomac.1c01635
Biomacromolecules 2022, 23, 1703−1712

viability at 2.5 μM to ~0% viability at 12.5 μM (Figure 2b). In sharp contrast, incubation with NPC 3 provided essentially complete cell viability over the entire concentration range tested with only a modest reduction in cell viability to 94 ± 4% observed at 25 μM. These results taken together provide additional support for the neuroprotective properties of NPC 3. Further evidence supporting this hypothesis was provided by direct visualization of SH-SY5Y cell viability via confocal microscopy. Here, SH-SY5Y cell were incubated with acrolein with or without the NPC 3 (0.3 mg mL^{-1}) for 18 h. The cells were then stained with Hoescht nuclear stain (blue) and galectin-3 antibody (green) to label the cell membrane. As can be observed in Figure 2c, cells incubated with acrolein alone (25 μM) show morphologies that were consistent with apoptosis, while cells that were co-incubated with the copolymer (0.3 mg mL^{-1}) (Figure 2d) show morphologies that are similar to those of the untreated control (Figure 2e).

3.4. In Vivo Studies. To evaluate how the protective effects of NPC 3 observed in vitro might translate to an animal model, DCE-MRI was performed to assess brain uptake and accumulation in a CCI mouse model of TBI. Gd-based compounds are widely used to provide positive MRI contrast in both preclinical and clinical settings.[24] Gd was incorporated into NPC 3 in order to provide contrast enhancement and allow accumulation and retention of the copolymer in the brain to be followed. Here, a polymerizable methacrylate monomer (ProbMer) containing a Gd-DOTA group (GdMA) was synthesized from cyclen in order to eliminate the need for costly and time-consuming post-polymerization conjugation reactions. Characterization of contrast enhancement at 9.4T showed T1 and T2 relaxivities of 3.05 and 8.21 s^{-1} mM^{-1}, respectively, and an r2/r1 of 2.69. These values suggest the viability of the compound for T1 enhancement as they are within the range of Gd-DTPA, a clinically used agent, whose T1 relaxivity is 4.1 s^{-1} mM^{-1} at 9.4 T and r2/r1 is 1.12.[25] DCE-MRI was performed to estimate the volume transfer coefficient, K^{trans}, in the injured brain. K^{trans} describes the rate at which the contrast agent moves from the plasma into tissue and has been used previously to describe permeation across the disrupted BBB and in TBI mice.[25,26] K^{trans} mapping (Figure 3a,b) showed significantly higher permeation (p = 0.0097) in the injured region (mean K^{trans} = 0.049) compared with the contralateral hemisphere (mean K^{trans} = 0.0026). This observation of higher and more rapid uptake in the injured region combined with the ROS neutralization and cell viability data suggests the potential for treatment of elevated ROS in the injured region with minimal off-target effects to the surrounding brain. Based on these data suggesting delivery to the brain, further in vivo testing was carried out to determine the antioxidant effect in the injured brain.

NPC 3 was next tested in our CCI mice to evaluate the ability of the copolymer to reduce the spread of ROS following a CCI. Based on the MRI studies, which showed that NPC 3 passively accumulates and is retained in the brain injury following CCI (Figure 3a,b), mice were injected through the tail vein with 100 μL of NPC 3 at 2 mg/mL (8 mg/kg body weight) in DPBS immediately after impact. This provided an NPC 3 concentration of approximately 0.1 mg/mL in the blood. As a positive control, a well-known small antioxidant molecule, MnTMPyP, was employed.[30,31] MnTMPyP is a cell permeable SOD/catalase mimetic that possesses the catalytic activity of both enzymes. Here, 500 μL of MnTMPyP at 1 mg/mL (20 mg/kg body weight) in DPBS was injected

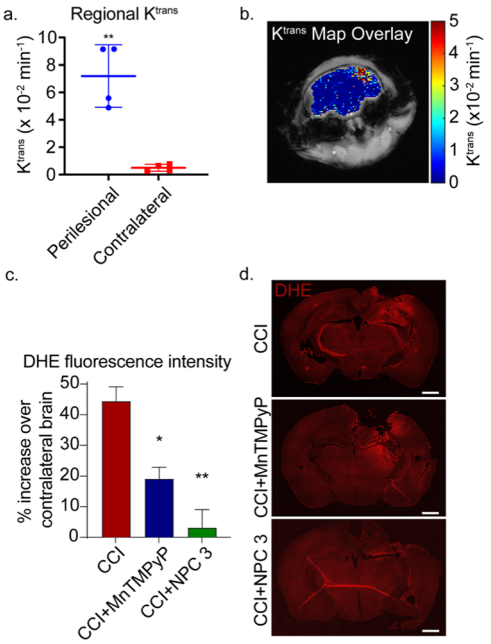

Figure 3. (a,b) In vivo DCE-MRI and K^{trans} mapping of mice 3 h post-injury. (a) Significantly higher K^{trans} was observed in the ipsilateral region compared with the contralateral region (p = 0.0097) as determined by a paired t-test. (b) The K^{trans} map shows that higher permeability (red) corresponds with the ipsilateral region (right side of the brain in the image), while lower values are observed in the contralateral hemisphere. (c,d) In vivo DHE staining of the brains at 4 h post-injury. (c) DHE fluorescence mean intensity at the perilesional normalized to the contralateral hemisphere. Data are shown as mean ± SEM with n = 3 for each treatment group; 1.439 ± 0.055 for untreated CCI mice, 1.189 ± 0.045 for MnTMPyP-treated CCI mice, and 1.032 ± 0.071 for NPC 3-treated CCI mice. * indicates a statistical difference compared to control, with one and two symbols indicating p < 0.05 and p < 0.01, respectively, as determined by one-way ANOVA and Tukey's post hoc test. (d) Representative images of the DHE staining of the untreated CCI mice, MnTMPyP-treated CCI mice, and NPC 3-treated CCI mice. The scale bar is 1000 μm.

intraperitoneally immediately after impact to maximally reduce ROS levels at this dose.[32]

A DHE assay was then employed to observe the spread of ROS in the acute phase of the injury (4 h post-CCI). DHE becomes fluorescent when oxidized by ROS, providing a convenient method for visualizing ROS levels in vivo. Because ROS are common signaling molecules in the brain and are produced as a byproduct of ATP production,[29] some DHE fluorescence is expected in the brain under physiological conditions. Therefore, the fluorescence intensity in the perilesional tissue was normalized to the contralateral hemisphere to reduce the variation in the base ROS in individual mice as well as to show the increase in ROS in the perilesional tissue. DHE fluorescence was highly increased in the perilesional area in CCI mice, which was reduced by treatments with MnTMPyP and NPC 3 (Figure 3c).

Quantifying these fluorescence levels across all animals (Figure 3d) revealed that CCI mice had an approximately 43.9% increase in DHE fluorescence in the perilesional area as compared to the contralateral brain (normalized DHE fluorescence of 1.439 ± 0.055). MnTMPyP significantly reduced DHE fluorescence to an 18.9% increase over the contralateral brain (normalized DHE fluorescence of 1.189 ±

https://doi.org/10.1021/acs.biomac.1c01635
Biomacromolecules 2022, 23, 1703−1712

0.045). In comparison, NPC 3 provided nearly complete protected of the perilesional area, showing a 3.2% increase over the contralateral brain (normalized DHE fluorescence of 1.032 ± 0.071). These results indicated that NPC 3 significantly reduced the spread of ROS in the acute phase of the injury compared to the untreated CCI mice. NPC 3 also seems to be more effective in reducing ROS compared to the small antioxidant molecule, MnTMPyP, which also significantly reduces the ROS compared to the untreated CCI mice. Thus, the in vivo DHE assay supports our in vitro findings that NPC 3 provides robust neuroprotective properties within 4 h of NP injection in the CCI mouse model of TBI.

4. CONCLUSIONS

A series of thiol-functionalized, water-soluble copolymers were synthesized for the targeted neutralization of ROS and LPOx. HRPO-H_2O_2 assays showed that NPC 3 was able to efficiently neutralize H_2O_2. The antioxidant properties of NPC 3 were further supported by RPE assays, which demonstrated the ability of the copolymer to protect the ROS-sensitive protein from oxidation. Direct evidence for the ability of NPC 3 to covalently react with acrolein was provided by $_1$H NMR studies, which showed that the copolymer rapidly and quantitatively reacts with electron-deficient LPOx. These results combined with in vitro cytotoxicity experiments conducted with SH-SY5Y differentiated neurons showed that NPC 3 provides substantial protection against acrolein. These findings were further supported by direct evaluation of cell morphology via confocal morphology where cells incubated with NPC 3 and acrolein showed morphologies similar to the untreated cells, while morphologies consistent with apoptosis were observed for the acrolein alone samples. Direct in vivo visualization of the theranostic copolymers via MRI demonstrated the passive accumulation and retention of these materials in a mouse model of TBI. Additionally, DHE assays showed that NPC 3 significantly reduces the spread of biochemical derangements in mice at 4 h post-CCI. This suggests that these materials may function well to reduce multiple mechanisms of secondary injury following TBI.

■ ASSOCIATED CONTENT

Supporting Information

The Supporting Information is available free of charge at https://pubs.acs.org/doi/10.1021/acs.biomac.1c01635.

Synthesis of mon(LIPOMA) from α-LA; synthesis of mon(GdMA), TRI-BOC, SMA Cl, BOC DOTA, and GdMA; L-cysteine standard curve for NPC series thiol quantification; standardizing RPE protein assay using AAPH; verification of ^{1}H NMR acrolein neutralization method using DHLA; determination of toxicity curves for reduced NPC 3 copolymer, H_2O_2, and acrolein; 1H NMR and 13C NMR spectra for LIPOMA monomer; 1H NMR data for BOC DOTA; 1H NMR for deprotected DOTA; 1H NMR for GdMA; GPC traces for NPCs 1, 2, and 3; Ellman's reagent assay thiol concentration results; and cytotoxicty curves for reduced NPC 3 copolymer, acrolein, and peroxide (PDF)

■ AUTHOR INFORMATION

Corresponding Author

Anthony J. Convertine − *Department of Material Science and Engineering, Missouri University of Science and Technology, Rolla, Missouri 65409, United States;* orcid.org/0000-0002-3263-1523; Email: convertinea@mst.edu

Authors

Aaron Priester − *Department of Material Science and Engineering, Missouri University of Science and Technology, Rolla, Missouri 65409, United States*

Richard Waters − *Department of Material Science and Engineering, Missouri University of Science and Technology, Rolla, Missouri 65409, United States*

Ashleigh Abbott − *Department of Material Science and Engineering, Missouri University of Science and Technology, Rolla, Missouri 65409, United States*

Krista Hilmas − *Department of Material Science and Engineering, Missouri University of Science and Technology, Rolla, Missouri 65409, United States*

Klaus Woelk − *Department of Material Science and Engineering, Missouri University of Science and Technology, Rolla, Missouri 65409, United States;* orcid.org/0000-0002-1386-5623

Hunter A. Miller − *Department of Biological Systems Engineering, University of Nebraska-Lincoln, Lincoln, Nebraska 68583-0900, United States*

Aria W. Tarudji − *Department of Biological Systems Engineering, University of Nebraska-Lincoln, Lincoln, Nebraska 68583-0900, United States*

Connor C. Gee − *Department of Biological Systems Engineering, University of Nebraska-Lincoln, Lincoln, Nebraska 68583-0900, United States*

Brandon McDonald − *Department of Biological Systems Engineering, University of Nebraska-Lincoln, Lincoln, Nebraska 68583-0900, United States*

Forrest M. Kievit − *Department of Biological Systems Engineering, University of Nebraska-Lincoln, Lincoln, Nebraska 68583-0900, United States;* orcid.org/0000-0002-9847-783X

Complete contact information is available at: https://pubs.acs.org/10.1021/acs.biomac.1c01635

Author Contributions

The manuscript was written through contributions of all authors. All authors have given approval to the final version of the manuscript.

Funding

F.K. acknowledges support from the National Institute of Neurological Disorders and Stroke of the National Institutes of Health (R01NS109488). We would also like to acknowledge support from the Missouri S&T Center for Biomedical Research.

Notes

The authors declare no competing financial interest.

■ ACKNOWLEDGMENTS

We acknowledge the Nano-Engineering Research Core facility supported by the Nebraska Research Initiative fund for use of the confocal microscope. We thank Richard Watters for assistance with cell culture work. We thank Dr. Katie Shannon for assistance with optical imaging of cells.

■ ABBREVIATIONS

CCR2, CC chemokine receptor 2; CCL2, CC chemokine ligand 2; CCR5, CC chemokine receptor 5; TLC, thin layer

chromatography; TBI, traumatic brain injury; ROS, reactive oxygen species; LPOx, lipid peroxidation product; 4HNE, 4-hydroxynonenal; LIPOMA, lipoic acid methacrylate; O950, polyethylene glycol monomethyl ether methacrylate; DOTA, 2,2′,2″,2‴-(1,4,7,10-tetraazacyclododecane-1,4,7,10-tetrayl)-tetraacetic acid; MRI, magnetic resonance imaging; NPCs, neuroprotective copolymers; RAFT, reversible addition−fragmentation chain transfer; CCI, controlled cortical impact; LA, lipoic acid; DHLA, $[M]_o$:$[CTA]_o$, dihydrolipoic acid; initial monomer-to-chain transfer agent ratio; $[CTA]_o$:$[I]_o$, initial chain transfer agent to initiator ratio; PBS, phosphate buffered saline; DLS, dynamic light scattering; HRPO, horseradish peroxidase; RPE, R-phycoerythrin; ProbMer, polymerizable methacrylate monomer; DHE, dihydroethidium

REFERENCES

(1) Taylor, C. A.; Bell, J. M.; Breiding, M. J.; Xu, L. Traumatic Brain Injury-Related Emergency Department Visits, Hospitalizations, and Deaths - United States, 2007 and 2013. *MMWR Surveill. Summ.* **2017**, *66*, 1−16.

(2) McInnes, K.; Friesen, C. L.; MacKenzie, D. E.; Westwood, D. A.; Boe, S. G. Correction: Mild Traumatic Brain Injury (mTBI) and Chronic Cognitive Impairment: a Scoping Review. *PLoS One* **2019**, *14*, No. e0218423.

(3) Mortezaee, K.; Khanlarkhani, N.; Beyer, C.; Zendedel, A. Inflammasome: Its Role in Traumatic Brain and Spinal Cord Injury. *J. Cell. Physiol.* **2018**, *233*, 5160−5169.

(4) Ladak, A. A.; Enam, S. A.; Ibrahim, M. T. A Review of the Molecular Mechanisms of Traumatic Brain Injury. *World Neurosurg.* **2019**, *131*, 126−132.

(5) Liddelow, S. A.; Guttenplan, K. A.; Clarke, L. E.; Bennett, F. C.; Bohlen, C. J.; Schirmer, L.; Bennett, M. L.; Münch, A. E.; Chung, W.-S.; Peterson, T. C.; et al. Neurotoxic Reactive Astrocytes Are Induced by Activated Microglia. *Nature* **2017**, *541*, 481−487.

(6) Hadass, O.; Tomlinson, B. N.; Gooyit, M.; Chen, S.; Purdy, J. J.; Walker, J. M.; Zhang, C.; Giritharan, A. B.; Purnell, W.; Robinson, C. R.; et al. Selective Inhibition of Matrix Metalloproteinase-9 Attenuates Secondary Damage Resulting From Severe Traumatic Brain Injury. *PLoS One* **2013**, *8*, No. e76904.

(7) Mohamadpour, M.; Whitney, K.; Bergold, P. J. The Importance of Therapeutic Time Window in the Treatment of Traumatic Brain Injury. *Front. Neurosci.* **2019**, *13*, 07.

(8) Di Pietro, V.; Yakoub, K. M.; Caruso, G.; Lazzarino, G.; Signoretti, S.; Barbey, A. K.; Tavazzi, B.; Lazzarino, G.; Belli, A.; Amorini, A. M. Antioxidant Therapies in Traumatic Brain Injury. *Antioxidants* **2020**, *9*, 260.

(9) Hall, E. D.; Wang, J. A.; Miller, D. M.; Cebak, J. E.; Hill, R. L. Newer Pharmacological Approaches for Antioxidant Neuroprotection in Traumatic Brain Injury. *Neuropharmacology* **2019**, *145*, 247−258.

(10) Gruenbaum, S. E.; Zlotnik, A.; Gruenbaum, B. F.; Hersey, D.; Bilotta, F. Pharmacologic Neuroprotection for Functional Outcomes After Traumatic Brain Injury: a Systematic Review of the Clinical Literature. *CNS Drugs* **2016**, *30*, 791−806.

(11) Reddy, M. K.; Labhasetwar, V. Nanoparticle-mediated delivery of superoxide dismutase to the brain: an effective strategy to reduce ischemia-reperfusion injury. *FASEB J.* **2009**, *23*, 1384−1395.

(12) Liu, T. H.; Beckman, J. S.; Freeman, B. A.; Hogan, E. L.; Hsu, C. Y. Polyethylene Glycol-Conjugated Superoxide Dismutase and Catalase Reduce Ischemic Brain Injury. *Am. J. Physiol.* **1989**, *256*, H589−H593.

(13) Marshall, L. F.; Maas, A. I. R.; Marshall, S. B.; Bricolo, A.; Fearnside, M.; Iannotti, F.; Klauber, M. R.; Lagarrigue, J.; Lobato, R.; Persson, L.; et al. A Multicenter Trial on the Efficacy of Using Tirilazad Mesylate in Cases of Head Injury. *J. Neurosurg.* **1998**, *89*, 519−525.

(14) Tarudji, A. W.; Gee, C. C.; Romereim, S. M.; Convertine, A. J.; Kievit, F. M. Antioxidant Thioether Core-Crosslinked Nanoparticles Prevent the Bilateral Spread of Secondary Injury to Protect Spatial Learning and Memory in a Controlled Cortical Impact Mouse Model of Traumatic Brain Injury. *Biomaterials* **2021**, *272*, 120766.

(15) Yoo, D.; Magsam, A. W.; Kelly, A. M.; Stayton, P. S.; Kievit, F. M.; Convertine, A. J. Core-Cross-Linked Nanoparticles Reduce Neuroinflammation and Improve Outcome in a Mouse Model of Traumatic Brain Injury. *ACS Nano* **2017**, *11*, 8600−8611.

(16) Xu, J.; Ypma, M.; Chiarelli, P. A.; Park, J.; Ellenbogen, R. G.; Stayton, P. S.; Mourad, P. D.; Lee, D.; Convertine, A. J.; Kievit, F. M. Theranostic Oxygen Reactive Polymers for Treatment of Traumatic Brain Injury. *Adv. Funct. Mater.* **2016**, *26*, 4124−4133.

(17) Ferrari, R.; Ceconi, C.; Curello, S.; Cargnoni, A.; Alfieri, O.; Pardini, A.; Marzollo, P.; Visioli, O. Oxygen Free Radicals and Myocardial Damage: Protective Role of Thiol-Containing Agents. *Am. J. Med.* **1991**, *91*, 95S−105S.

(18) Chan, J. W.; Hoyle, C. E.; Lowe, A. B.; Bowman, M. Nucleophile-Initiated Thiol-Michael Reactions: Effect of Organo-catalyst, Thiol, and Ene. *Biomacromolecules* **2010**, *43*, 6381−6388.

(19) Packer, L.; Witt, E. H.; Tritschler, H. J. Alpha-Lipoic Acid as a Biological Antioxidant. *Free Radic. Biol. Med.* **1995**, *19*, 227−250.

(20) Schönheit, K.; Gille, L.; Nohl, H. Effect of Alpha-Lipoic Acid and Dihydrolipoic Acid on Ischemia/Reperfusion Injury of the Heart and Heart Mitochondria. *Biochim. Biophys. Acta* **1995**, *1271*, 335−342.

(21) Roy, D.; Berguig, G. Y.; Ghosn, B.; Lane, D. D.; Braswell, S.; Stayton, P. S.; Convertine, A. J. Synthesis and Characterization of Transferrin-Targeted Chemotherapeutic Delivery Systems Prepared via RAFT Copolymerization of High Molecular Weight PEG Macromonomers. *Polym. Chem.* **2014**, *5*, 1791−1799.

(22) Das, D.; Srinivasan, S.; Kelly, A. M.; Chiu, D. Y.; Daugherty, B. K.; Ratner, D. M.; Stayton, P. S.; Convertine, A. J. RAFT Polymerization of Ciprofloxacin Prodrug Monomers for the Controlled Intracellular Delivery of Antibiotics. *Polym. Chem.* **2016**, *7*, 826−837.

(23) Das, D.; Chen, J.; Srinivasan, S.; Kelly, A. M.; Lee, B.; Son, H.-N.; Radella, F.; West, T. E.; Ratner, D. M.; Convertine, A. J.; et al. Synthetic Macromolecular Antibiotic Platform for Inhalable Therapy Against Aerosolized Intracellular Alveolar Infections. *Mol. Pharm.* **2017**, *14*, 1988−1997.

(24) Bellin, M.-F. MR contrast agents, the old and the new. *Eur. J. Radiol.* **2006**, *60*, 314−323.

(25) Miller, H. A.; Magsam, A. W.; Tarudji, A. W.; Romanova, S.; Weber, L.; Gee, C. C.; Madsen, G. L.; Bronich, T. K.; Kievit, F. M. Evaluating Differential Nanoparticle Accumulation and Retention Kinetics in a Mouse Model of Traumatic Brain Injury via Ktrans Mapping with MRI. *Sci. Rep.* **2019**, *9*, 16099−16114.

(26) Montagne, A.; Barnes, S. R.; Sweeney, M. D.; Halliday, M. R.; Sagare, A. P.; Zhao, Z.; Toga, A. W.; Jacobs, R. E.; Liu, C. Y.; Amezcua, L.; et al. Blood-Brain Barrier Breakdown in the Aging Human Hippocampus. *Neuron* **2015**, *85*, 296−302.

(27) Reiner, C. K.; Kada, G.; Gruber, H. J. Quick Measurement of Protein Sulfylhydryls with Ellman's Reagent and with 4,4'-Dithiodipyridine. *Anal. Bioanal. Chem.* **2002**, *373*, 266−276.

(28) Pick, E.; Keisari, Y. A Simple Colorimetric Method for the Measurement of Hydrogen Peroxide Produced by Cells in Culture. *J. Immunol. Methods* **1980**, *38*, 161−170.

(29) Glazer, A. N. [14] Phycoerythrin fluorescence-based assay for reactive oxygen species. *Methods Enzymol.* **1990**, *186*, 161−168.

(30) Wang, X.; Sun, D.; Hu, Y.; Xu, X.; Jiang, W.; Shang, H.; Cui, D. The Roles of Oxidative Stress and Beclin-1 in the Autophagosome Clearance Impairment Triggered by Cardiac Arrest. *Free Radic. Biol. Med.* **2019**, *136*, 87−95.

(31) Nair, A.; Jacob, S. A Simple Practice Guide for Dose Conversion Between Animals and Human. *J. Basic Clin. Pharmacol.* **2016**, *7*, 27−31.

(32) Beckhauser, T. F.; Francis-Oliveira, J.; De Pasquale, R. Reactive Oxygen Species: Physiological and Physiopathological Effects on Synaptic Plasticity. *J. Exp. Neurosci.* **2016**, *10*, 23−48.

https://doi.org/10.1021/acs.biomac.1c01635
Biomacromolecules 2022, 23, 1703−1712